

## **Selected aspects of the use of thermal & derivative analysis to improve macro modeling of solidification for casting iron. Comparison of chosen simulation codes**

**Zenon Ignaszak<sup>1\*</sup>, Esteban Codina<sup>2</sup>, Jakub Hajkowski<sup>1</sup>, Paweł Popielarski<sup>1</sup>, Pedro Roquet<sup>3</sup>**

<sup>1</sup>Poznan University of Technology, 3 Piotrowo street, 60-965 Poznan, Poland

<sup>2</sup>UPC Labson, Campus Terrassa, Colom, 11, 08222 Terrassa, Barcelona, Spain

<sup>3</sup>Fundiciones de Roda, Disseminats, s/n, Roda de Ter, Spain

The article concerns the influence of grey cast iron density and different trials of fraction of solid curves (influencing latent heat generation) on the formation of shrinkage discontinuities. Two alternatives of density curves were considered ( $\rho=f(T)$ ): the classical one, (usually applied in macro model simulation codes) and the modified one, which includes graphite expansion (based on compensation of primary shrinkage discontinuities during eutectic phase crystallization). Solid fraction curves applying Newtonian Thermal Analysis (NTA) were estimated. The experimental and numerical simulation tests were performed on the castings, which were made with Derivative Thermal Analysis (DerTA) standard cups and in furan-bonded sand cube mould of 250 mm side and a upper riser  $\phi 140 \times 200$  mm. The numerical tests were realized using NovaFlow&Solid (NF&S) and ProCast codes. Also, some tests were realized using ProCast with a micro model (default value parameters). In this work, the coupled influence of both curves on the dynamics of the shrinkage-expansion phenomena and on shrinkage defects prognosis in grey cast iron castings has been revealed.

**Keywords:** cast iron, simulation codes, macro/micro models, heat source function, porosity defects

### **Introduction**

The defects related to shrinkage remain one of the biggest quality problems. The application of foundry simulation codes in industrial conditions should, above all, ensure the most accurate predictions of casting quality. Only in this case, a proper assessment with criteria of minimum defects related to shrinkage can be stated. This item and the effectiveness of simulation codes using these criteria are the main challenges, regardless of its origin, discretization method and particular user's opinions.

Metal alloys crystallization phenomena simulation is based on mathematical models, which represent the complexity related with physical and chemical processes in a very diversified way. The corresponding simplifications are assigned to applied simulation code and must be taken into consideration in database. The coefficients for the database should be determined by experimental validation by comparing the real and virtual casting process. Sometimes, the analysis can be difficult because the applied simplifications are not usually revealed to the users or not well described in the trouble-shooter (manual or help window in simulation code)<sup>1</sup>.

In the literature, problems of determination or validation of databases is named the inverse problem solution. The authors have devoted many of their previous publications on this topic.<sup>1,2,3,4</sup> Other authors discussed the problem of using more complex models through introducing a new phenomena, which can lead to better formal physical description, for example, nucleation of particular phases, their growth, including intermetallic phases, segregation, shrinkage and stress, and flow in the solid-liquid zone. Despite getting a quasi-ideal model, it is necessary the use of some simplifications and/or empirical models.<sup>1</sup> This is strictly related to a need of disposing the new physical parameters and coefficients (contained in a set of boundary conditions in the material databases), as shown in papers<sup>5,6</sup>. Nevertheless, not all parameters used in simplified models can be used in the complex ones, which is supposed to describe a real casting-mould system in a better way e.g. macro/micro models.

The phenomena, which are the most important in casting processes models, are shrinkage phenomena, compensation (decreasing) by a liquid metal stream, and void micro spaces refilling, which are related to the following items: feeding shrinkage coefficient (shrinkage of overheating and solidification), feeding flow range from the riser head, chills on the oriented (directional) solidification and casting configuration (dimensions and shape). All them are well known by casting process designers. The basic expectation, formulated through virtual simulation models (using preliminary technology concept), is the validation of its correctness regarding the shrinkage defects. The prognosis of these defects and its

---

\* Corresponding autor, e-mail: zenon.ignaszak@put.poznan.pl

comparison with acceptability criteria (formulated in the customer requirements), is a decisive factor in order to accept/refuse castings to be produced using the preliminary technology concept or after its optimization.

Shrinkage phenomena intensity is a result of density and crystallizing phases variability with temperature  $\rho=f(T)$ . On the other hand, dynamics of the solid phase generation (particular phases), flow conditions (so-called critical fraction of solid phase – critical  $F_s$ ) and gravity field will also decide the macro- and micro- shrinkage porosities (location and intensity).

This paper presents the application of the Derivative Thermal Analysis (DerTA) of the grey cast iron castings (EN-GJL-250), poured in a standard DerTA cup (single thermocouple), in order to determine the solid fraction curve,  $F_s=f(T)$  used in a basic model of generation of the latent heat (macro model). Cooling curve shape in this method is a relatively easy way to obtain information about the crystallization process evolution. Simplified crystallization model has been used by simulation codes for a long time (solidification interpreted as an accumulative growth of the solid phase). Someone still use them (e.g. NF&S). Other codes use a new micro model (alternatively with macro model). A question appears – can the phenomena description in the macro model and the solid fraction curve  $F_s=f(T)$  enhance the prognosis of the grey cast iron castings shrinkage defects?

The method evaluates crystallization latent heat effects on the basis of temporal cooling curve derivative and „zero curve”,  $Z_N$ . For a real experimental sample, the difference between them explains the dynamics of the crystallization process. In this paper, „zero curve” has been estimated through a Newtonian Thermal Analysis (NTA). In NTA standard method,  $Z_N$  „zero curve” is arbitrarily defined by extrapolation of an exponential curve  $dT/dt = -A \exp(-Bt)$ , where  $dT/dt$  is cooling rate,  $A$  and  $B$  are experimentally determined constants and the assumption of null temperature gradient through the section of DerTA cup. „Zero curves” does not take into account the phase transition latent heat.

Liquid alloy temperature fields is described by the Fourier-Kirchhoff equation with internal heat sources:  $\partial T/\partial t = \alpha \nabla^2 T + q_s/C_v$ , where  $\partial T/\partial t$  is metal cooling rate [K/s],  $\alpha$  is thermal diffusivity [ $m^2/s$ ],  $C_v$  is volumetric specific heat [ $J/m^3 K$ ],  $q_s$  is volumetric heat generated during solidification resulting from NTA method [ $W/m^3$ ]. Fourier-Kirchhoff equation can be transformed into the following form<sup>7,8</sup>:  $q_s = C_v(\partial T/\partial t - Z_N)$  and the Newtonian zero curve has the form:  $Z_N = q_{su}/C_v M$ , where  $q_{su}$  is partial heat flow from casting surface to ambient, assigned to accumulative cooling of casting [ $W/m^2$ ],  $M$  is thermal modulus [m] (ratio between volume and cooling surface).

Fras et al. paper<sup>7</sup>, related with Newton (NTA) and Fourier (FTA) analyses indicates the differences in approximations of zero curves, assigned to solidifying casting particular points. FTA analysis requires that the nucleation and growth phenomena must be based on an empirical model<sup>9,10,11,12</sup> (e.g. the Oldfield model or similar e.g. Rappaz, Boeri or KGT), which means that it allows a different approximation of „zero curve”, based on specific simplifications.

The installation of a second thermocouple in DerTA cup is not standard yet. This experimental version permits a simplified temperature gradient evaluation through the section of DerTA cup. Precise separation of both thermal effects: accumulation heat and latent heat, for diversified non-equilibrium solidification conditions is not feasible. That is why NTA analysis was assumed as standard in this paper.

## Experimental and numerical studies

The experimental and simulation tests were performed on the castings samples, which were made with DerTA standard cups (Fig. 1a) and in furan-bonded sand cube mould of 250 mm side and a upper riser  $\phi 140 \times 200$  mm (Fig 1b). Table 1 shows average EN-GJL-250 cast iron chemical composition.

In developing a macro model, a priori, phase growth rate calculation in each solidifying micro region of the casting (assigned to a given node) is based on local temperature drop in the given time step (according to the  $F_s=f(t)$  curve) but, due to observed undercooling and recalescence effects, this calculation is not possible to be taken into account directly. So, if solid fraction  $F_s = f(T)$  curve estimation is based on experimental DerTA curve, we first need to approximate the curve as shown in Fig. 2.

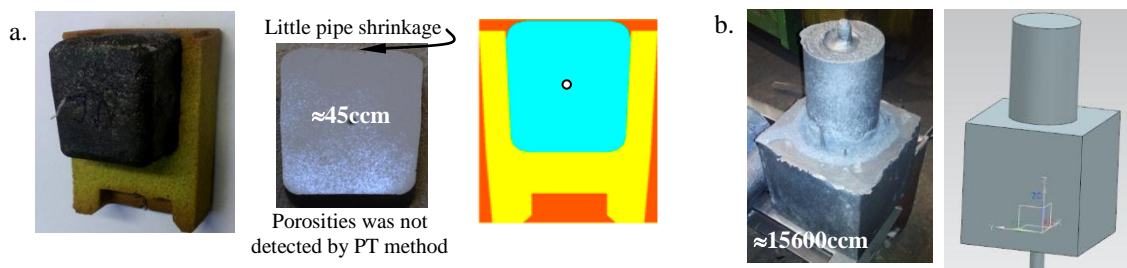


**Fig.1:** The views of the test EN-GJL 250 castings: a. standard DerTA cup (left), results of PT method after cutting (middle) and CAD geometry (right); b. real experimental cube casting (250 mm side) with upper riser  $\phi 140 \times 200$  mm (casting and CAD geometry).

Fig. 2a presents EN-GJL-250 alloy cooling curve and its first derivative selected from the test series carried out in Fundiciones de Roda facilities<sup>13</sup>, using the ITACA system developed by Proservice<sup>14</sup>. With these experimental data, calorimetric curves („zero curve”) were estimated using the NTA method,  $q_s=f(t)$  values were calculated using trapezoid scheme and finally  $F_s=f(T)$  curves were obtained (Fig.2b). The curve 1 represents the heat flow release  $q_s$ , but it cannot be introduced directly inside the macro model as a generated latent heat curve (its shape is due to undercooling and recalescence effects). Curves 2 and 3 represent broken linear approximation curves of the real solid fraction evolution considering a monotonic trend (cumulative  $F_s$  value increases as temperature decreases). Fig. 2b also contains others  $F_s=f(T)$  curves: curve 4 from the NF&S code and curve 5 from the ProCast code, both based on chemical analysis presented in Table 1. The values of the characteristic temperatures:  $T_{liq}$ ,  $T_{eut}$  and  $T_{sol}$  respectively by NF&S and ProCast own modules, were also calculated.

**Table 1:** Average chemical analysis [%] of the EN-GJL-250 cast iron used in the studies.

C	Si	Mn	Mg	P	S	Cu	Cr	Mo	Ni	V	Sn	Pb	Ti	Te	Ceq
2,93	2,01	0,82	0,00	0,02	0,06	1,24	0,04	0,00	0,02	0,00	0,00	0,00	0,02	0,00	3,61

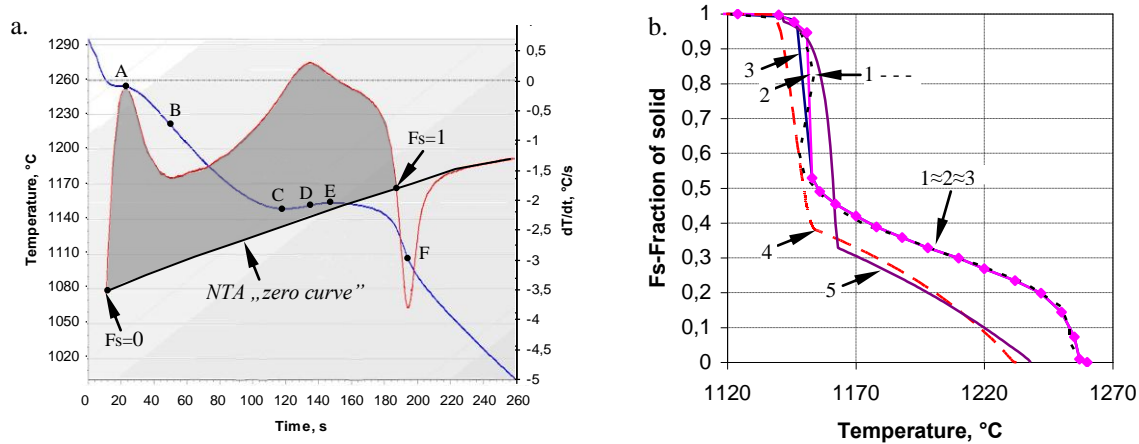


**Fig. 2a:** Cooling curve of grey cast iron type EN-GJL-250 and its first derivative obtained by DerTA cup method (ITACA<sup>14</sup>) with principle of „zero curve” determination. Characteristic temperature points [°C]: A-  $T_{Liq.}=1253$ ; B-  $T_{eut.Start}=1219$ ; C-  $T_{eut.Min}=1148$ ; D-  $T_{eut.Intermediate}=1152$ ; E-  $T_{eut.Max}=1154$ ; F-  $T_{Sol.}=1107$

**Fig. 2b:** Variation of solid fraction with temperature: 1 - curve (dashed) deduced from cooling curve showed in the Fig. 2a; 2 and 3 –simplified curves without the undercooling/recalescence; 4 and 5 – curves according to NF&S and ProCast databases respectively, both based on chemical analysis presented in Table 1. The maximal temperatures on the curves are the liquidus temperatures for cases 1 to 5.

Volume balance related to the shrinkage phenomena in a solidifying alloy is dependent on its density variation with the temperature. These phenomena in a liquid and solid-liquid state directly decide on the shrinkage defects formation. Most cast alloys are characterized by a continuous density increases as temperature decreases.

In the most databases regarding even the cast iron, the density variation character is preserved. However, it is known that the graphite crystallization as a graphite eutectic component is accompanied by the so-called graphite expansion (graphite volume growth), which must causes density decrease in defined temperature interval for case of the eutectic cast iron. This problem is rarely considered in the simulation system databases. Because of the above mentioned items, two  $\rho=f(T)$  curves were tested (the first considers a continuous density increases as temperature decreases-Fig.3b and the second considers a density decreases around of eutectic temperature due to eutectic graphite expansion-Fig.3c).

In relation with numerical tests for validation codes, critical liquid fractions parameters (CLF) limits for feeding flow have been formulated. In NF&S code, the limit levels are: mass feeding about 50% and inter-dendritic feeding (capillary) about 30%. Also, in ProCast code, mass feeding about 50% and inter-dendritic feeding about 70%.

In the numerical experiment tests, identical cast iron thermo-physical curves were assumed: heat conductivity and specific heat, (Fig. 3a). Also, constant latent heat value was considered (254 kJ/kg).

The thermo-physical parameters of sands (Croning sand cup and furan-bound sand cube) were assumed as constant values in temperature range of 20÷1500°C: heat conductivity were equal 0,8 and 1,04 W/m K respectively and the specific heat 1000 J/kg K and density 1540 kg/m<sup>3</sup> for both materials.

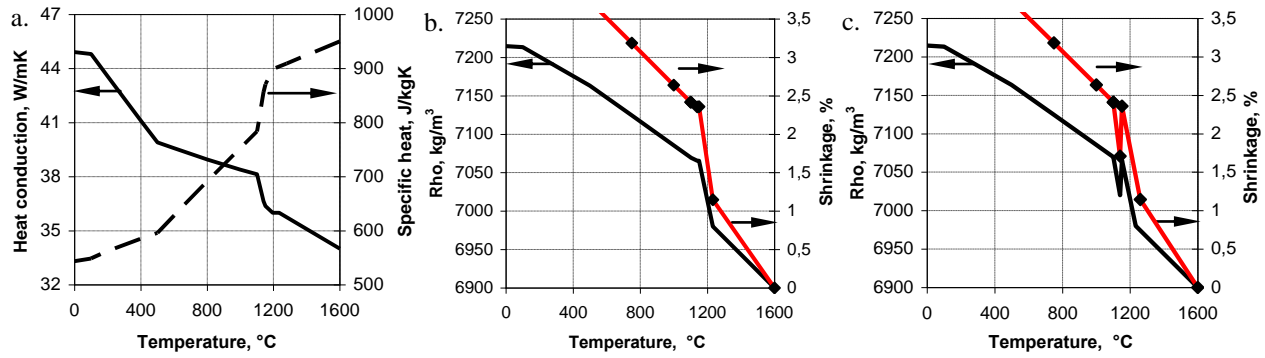


**Fig.3:** Chosen database parameters for EN-GJL-250 cast iron: a. heat conduction and specific heat, b. density and shrinkage curves in variant Rho 1 (without graphite expansion consideration), c. density and shrinkage curves in variant Rho 2 (with graphite expansion consideration).

### Results and discussion

Tables 2, 3 and 4 show simulation results obtained using two simulation codes and its comparison for the casting geometries: NF&S with Macro model and ProCast with Macro and Micro models. They are presented in form of a sequence for selected cooling time. Specific simulation variants are denominated by its solid fraction curve number (Fig. 2b – Fs 2, Fs3 and Fs 4) and its density curve number (Fig. 3b – Rho 1 and Fig. 3c – Rho 2).

**Table 2:** Chosen results sequence obtained from NovaFlow&Solid CV for different variants: Fs & Rho.

Variant: Fs 4 & Rho 1						
Liquid phase (Fl)	 Time: 0min:0s Σ Liq. phase: 100% Σ shrinkage: 0%	 Time: 0min:22s Σ Liq. phase: 91,6% Σ shrinkage: 0,7%	 Time: 0min:50,5s Σ Liq. phase: 69,5% Σ shrinkage: 1,4%	 Time: 1min:16s Σ Liq. phase: 51,7% Σ shrinkage: 1,52%	 Time: 2min:36s Σ Liq. phase: 9,9% Σ shrinkage: 1,53%	 Time: 3min:19s Σ Liq. phase: 0% Σ shrinkage: 1,54%
Shrinkage [%]	 Time: 0min:0s Σ Liq. phase: 100% Σ shrinkage: 0%	 Time: 0min:22s Σ Liq. phase: 91,6% Σ shrinkage: 0,7%	 Time: 0min:50,5s Σ Liq. phase: 69,5% Σ shrinkage: 1,4%	 Time: 1min:16s Σ Liq. phase: 51,7% Σ shrinkage: 1,52%	 Time: 2min:36s Σ Liq. phase: 9,9% Σ shrinkage: 1,53%	 Time: 3min:19s Σ Liq. phase: 0% Σ shrinkage: 1,54%
Variant: Fs 4 & Rho 2						
Shrinkage [%]	 Time: 0min:0s Σ Liq. phase: 100% Σ shrinkage: 0%	 Time: 0min:22s Σ Liq. phase: 91,6% Σ shrinkage: 1,05%	 Time: 0min:37s Σ Liq. phase: 79,5% Σ shrinkage: 1,3%	 Time: 1min:13s Σ Liq. phase: 53,8% Σ shrinkage: 0,9%	 Time: 1min:47s Σ Liq. phase: 34% Σ shrinkage: 0,73%	 Time: 3min:21s Σ Liq. phase: 0% Σ shrinkage: 1,54%
<p>Local value (indicated by arrows) of liquid phase fraction (Fl): 1,0 is equivalent to 100% Fl and respectively 0 to 0% Fl (obviously 100% Fl corresponds to 0% Fs and 0% Fl to 100% Fs). Local shrinkage values are also indicated by arrows. The description of each sequence contains for indicated value of the time: the remaining fraction [%] of the liquid phase (Σ Liquid phase) and the relative total shrinkage volume [%], including the possible expansion of graphite phase (Σ shrinkage).</p>						

Table 2 shows NF&S numerical simulation test results obtained using Fs 4 solid fraction curve and two density curves (Rho 1 and Rho 2). It can be seen progressive shrinkage volume increase. Contribution of Rho 2 is lower than Rho 1, remember that Rho 1 doesn't consider the graphite expansion. It should be mentioned that similar dependency is present on

ProCast simulation tests results but, in this case, internal shrinkage discontinuities were finally completely compensated by graphite expansion. Only the primary shrinkage (pipe) formed before eutectic crystallization on casting top side will be not compensated (Table 3).

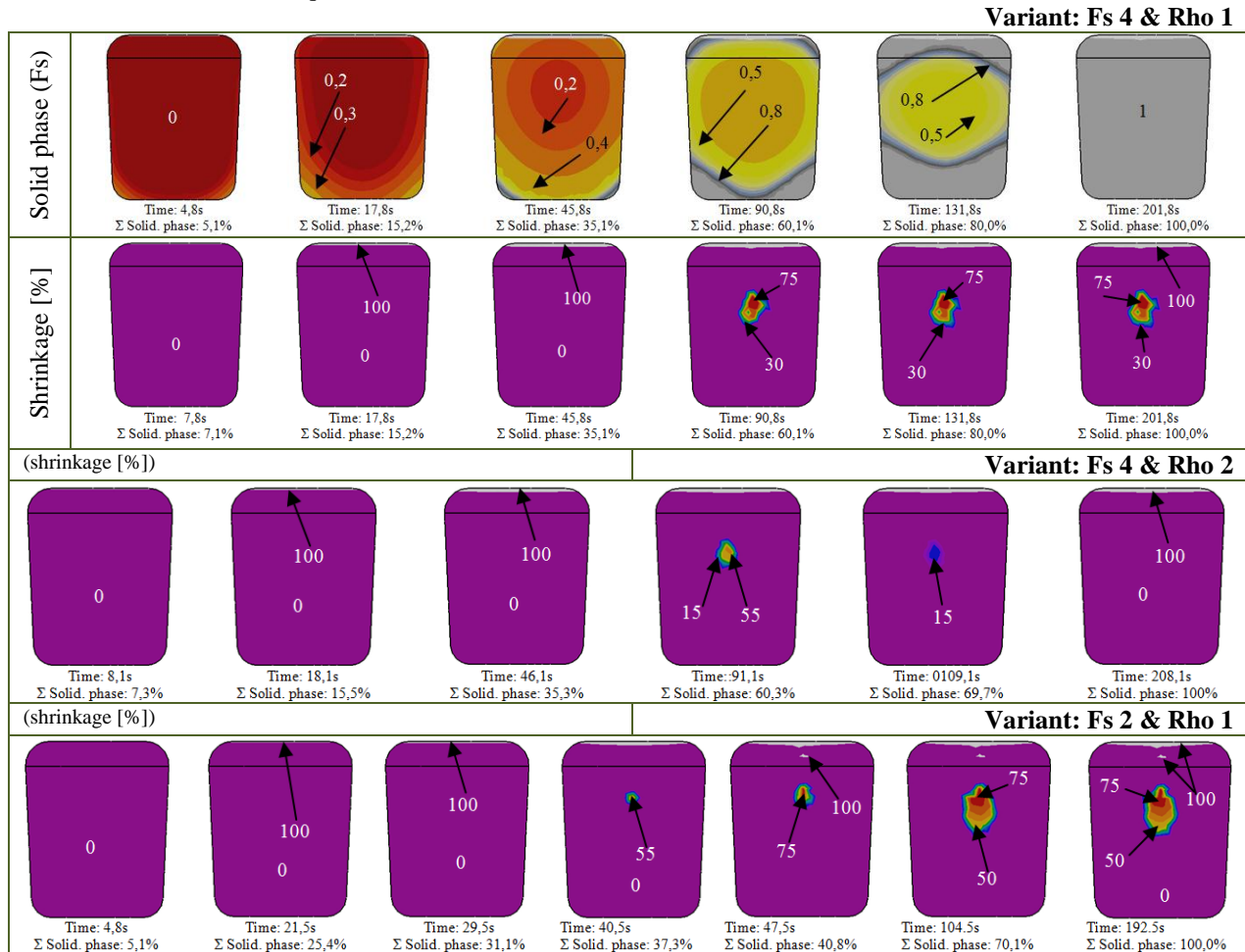
Comparing the results of Fs 4 & Rho 1 and Fs 2 & Rho 1 variants, we can see that second variant produces higher internal and pipe shrinkage. This is an evidence of solid influence on shrinkage defects. Also, these variants show full compensation of internal shrinkage defects but less shrinkage contribution can be observed before graphite expansion. Similar dependence occurs in Fs 3 & Rho 1 and Fs 3 & Rho 2 variants but with higher shrinkage contribution than variants before mentioned.

Results of ProCast numerical tests (Table 4), using its own micro model, show that its contribution in relation with internal shrinkage formation is much smaller than other variants. Also, compensation effect and highest primary shrinkage (pipe) intensity can be observed. Solid fraction variability with the temperature, assigned to a micro area (to a particular mesh node), has influence on the solidification process. If this  $F_s=f(T)$  variability is happening in the same temperature range  $T_{liq} - T_{sol}$ , there is practically no influence on simulated final solidification time. However, we need to make some assumptions about the use of the same database in relation to the remaining process parameters and materials, including the latent heat of solidification of the casting.

Changes of solid fraction curve profile, inside  $T_{liq} - T_{sol}$  range, with the above mentioned assumption, have influence on the solid phase growth evolution, which in turn affects the shrinkage-expansion processes in cast iron and local liquid phase micro flows feeding shrinkage cavities than have appeared.

In this study, the influence of  $Rho=f(T)$  and  $F_s=f(T)$  on predicted shrinkage porosities (distribution and quantity) was identified. The best porosity prediction between numerical and experimental tests has been observed by comparing the surface of DerTA cup casting cross-section (result obtained by penetration test, PT), shown in Fig. 1a, and ProCast numerical simulation results for Fs 4 & Rho 2 variant (Table 3). This good accordance was also confirmed by ProCast Micro model results (Table 4). Other trials for both codes (with other variants Fs-Rho) using Rho 2 have also given good results (minimal internal porosity), unlike those obtained using Rho 1.

**Table 3:** Chosen results sequence obtained from ProCast Macro model for different variants: Fs & Rho.



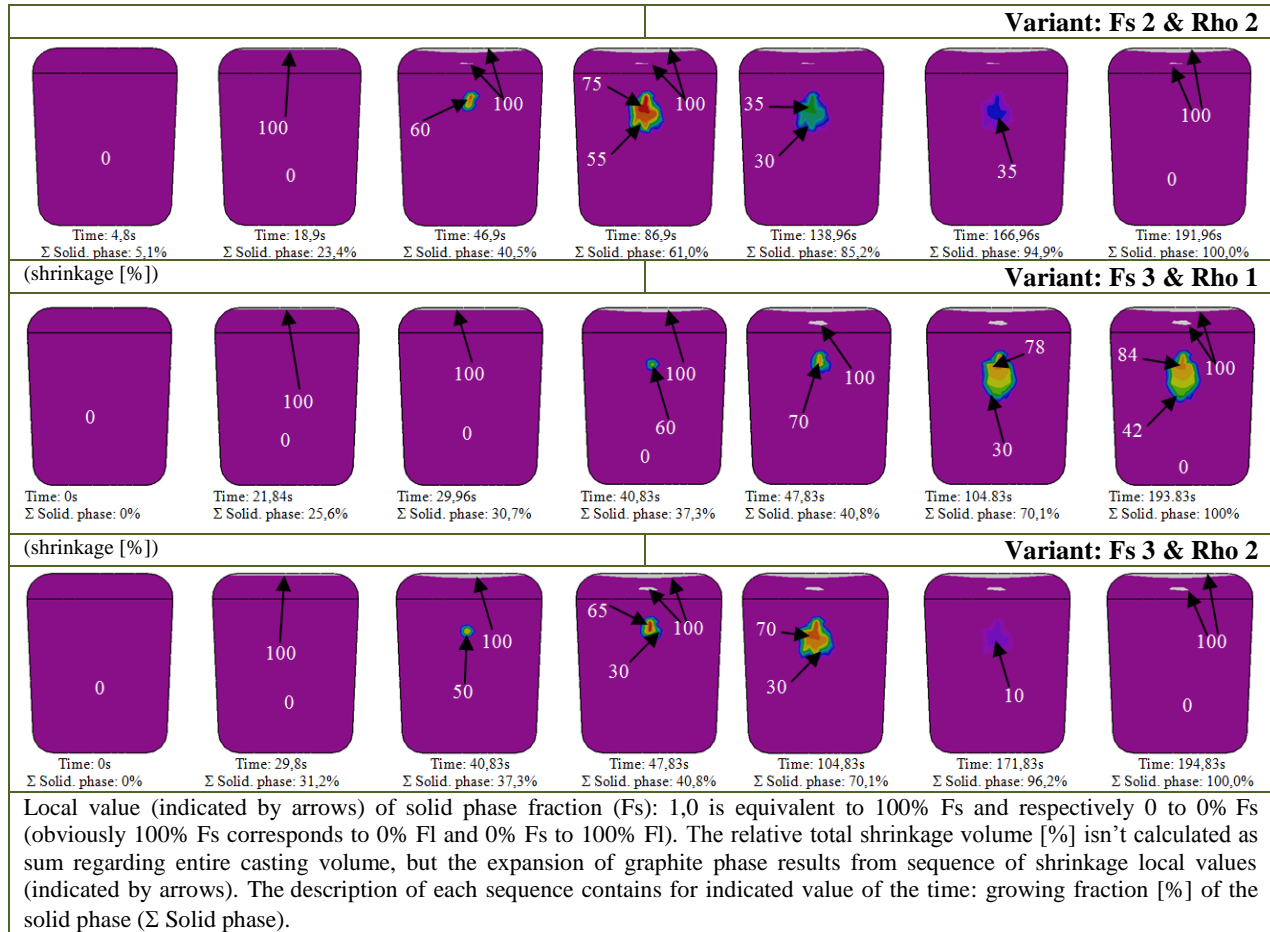
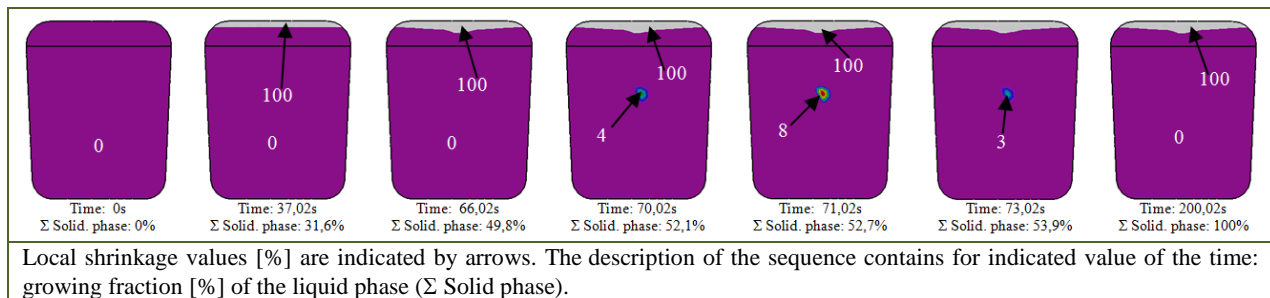


**Table 4:** Shrinkage sequence obtained from ProCast Micro model (to compare with Macro models).



Moreover, the application of the same thermal database parameters in both codes (NF&S and ProCast with Macro model) results in a different image related to porosity prognosis. This could be due to the hidden algorithms used by these commercial codes and therefore not available to users.

The same methodologies and, experimental and numerical tests were applied to evaluate coupled influence of  $F_s=f(T)$  and  $Rho=f(T)$  curve variants, in the  $T_{pouring} - T_{sol}$  range, over the shrinkage effects and expansion phenomena in relation with cube casting (approx. 15600 ccm) with the upper riser (Fig. 1b), so analogous to what was done with DerTA cup casting.

Table 5 shows final porosity prognosis results using both codes and selected variants. Shrinkage defects maps are different but when compared for example to Fs 4 and Rho 2 (cases c and e), we observed that these are unexpected. Some potential reasons were given in the previous deviation analysis realized for DerTA cup castings.

Fig. 4a shows the real surface of experimental cube casting cross-section (result obtained by PT test), which it is free of shrinkage defects. Pipe shrinkage occurred only in the top part of the riser. As can be seen from the results shown in Fig. 4b and 4c, only two variants of Fs & Rho showed an acceptable agreement with the experimental results (compare cases c and f from Table 5).

**Table 5:** Final shrinkage from NF&S CV (a,b,c) and ProCast (d,e,f) for chosen cases – cube casting (shrinkage %).

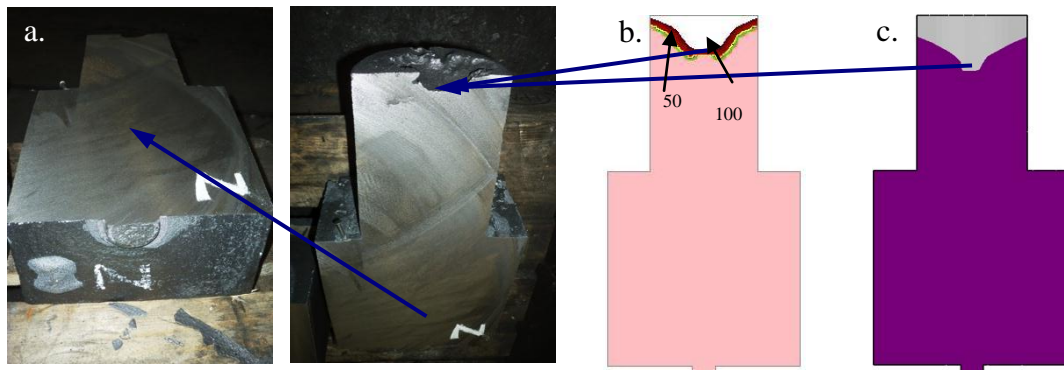
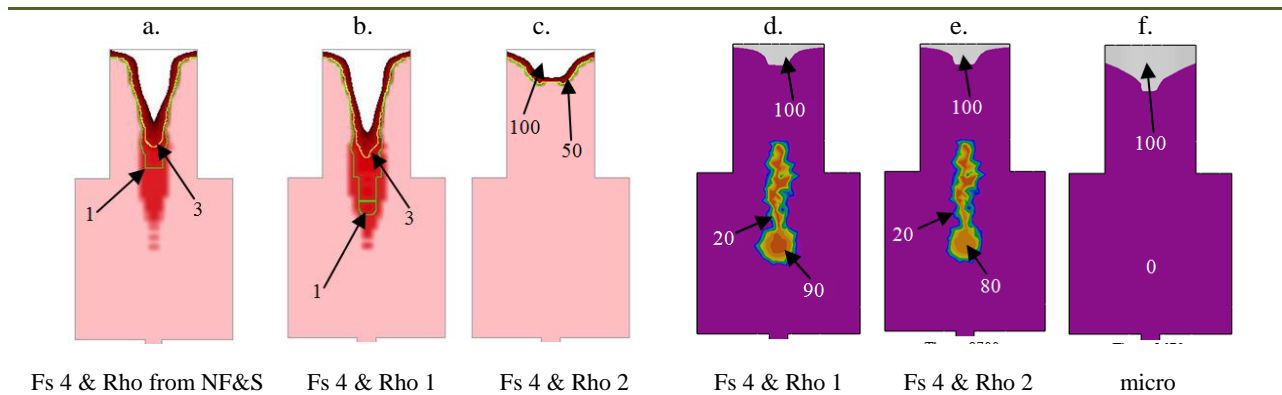


**Fig.4:** Correct soundness of real cube casting after cutting (a) compared with of shrinkage prognosis obtained from the NF&S CV Macro model (b) and from ProCast Micro model (c)

These results highlight the importance of the issues raised in this paper regarding a prognosis of shrinkage defects in cast iron castings. Also, one can recognize a certain influence on the castings size and shape.

## Conclusion

The tests performed in this study are related with an important problem concerning formation of shrinkage discontinuities phenomena in gray cast iron castings. Coupled shrinkage-expansion phenomena due to graphite phase increase do not exist in other technical alloys (e.g. cast steel, Al and Cu alloys etc.). These phenomena lead to shrinkage discontinuities reduction. This is the reason why these phenomena have been analyzed in this paper. Simulation tests using two codes and its macro models have been carry out. Also, other tests applying micro model (only with ProCast code) were realized. Generally, they confirm that is necessary to consider expansion-shrinkage phenomena modeling as well as an appropriate interpretation about dynamic shrinkage evolution during solidification process, before predicting a final casting shrinkage map.

To summarize the realized studies, the following remarks can be made:

1. Two simple casting geometries are used during experimental validation processes. More complicated casting shapes wouldn't allow an unequivocal answer regarding sensitivity analyses of simulation codes based on adequate databases selection (including hard and soft models<sup>1</sup>). Hence, the tests described in this paper let to prove the hypothesis with higher probability
2. Coupled influence of different variants about Fs and Rho curves on the shrinkage defects prediction for EN-GJL 250 castings, was confirmed.
3. Taking into account graphite expansion effect (Rho 2 curve), expected responses of both Macro models were observed.
4. ProCast's Micro model (some important shrinkage-expansion parameters are not available for users), gives satisfactory shrinkage predictions according both experimental castings.

Evaluation of experimental simulation tests efficiency using the macro or macro-micro models should definitely include the totality of castings quality. In the scope of these issues, we want to reflect that published numerical simulation studies using micro models, with extremely small casting sample size (cubic samples whose side is a fraction of a millimeter or 2D simple sample, e.g.<sup>15</sup>), are an important research area from the scientific viewpoint, which could be a practical significance in some undefined future. Prof. Rappaz<sup>16</sup> relates this area with microelectronics and computing developments and, in a visionary manner, considers that a full symbiosis with castings modeling, including the atomic scale, is likely to happen. On the one hand, there is need to find a coherent physical description of phenomena from the macro to atomic scale: basic differential equations (hard modeling) and empirical equations approach (soft modeling), but also, and on the other hand, maybe mostly, there is need to microelectronic developments and new computers generation (calculation speed and memory size). It should be considered that there are prognosis models<sup>16</sup> with working times even as long as 100 years.

## References

1. Z. Ignaszak: *Key Engineering Materials*, 2011, 457, 305-311.
2. Z. Ignaszak, P. Popielarski: *Archives of Foundry*, 2003, 3 (in Polish).
3. Z. Ignaszak, P. Popielarski, J. Ciura: *Archives of Foundry*, 2005, 5, 157-163.
4. Z. Ignaszak, P. Popielarski: *Archives of Foundry*, 2006, 6, 224-231 (in Polish).
5. Z. Ignaszak, J. Hajkowski, P. Popielarski: *Defect and Diffusion Forum*, 2013, 334-335, 314-321.
6. Z. Ignaszak, P. Popielarski, J. Hajkowski: *Defect and Diffusion Forum*, 2013, 336, 135-146.
7. E. Frás, W. Kapturkiewicz, A. Burbielko, H.F. Lopez: *AFS Trans.*, 1993, 101, 505-511.
8. A. Diószegi, I.L. Svensson, *Material Science and Engineering A*, 2005, A 413-414, 474-479.
9. D.J. Celentano, P.M. Dardati, L.A. Godoy, R.E. Boeri: *Int. J. Cast Met. Res.*, 2008, 21, 416-426.
10. Ch.-A. Gandin, M. Rappaz: *Acta Metall. Mater.*, 1994, 42, 2233-2246.
11. M. Rappaz, A. Jacot Ch.-A. Gandin: published in Raabe D.(editor) et all, *Continuum Scale Simulation of Engineering Materials Fundamentals - Microstructures - Process Applications*, Wiley-VCH 2004.
12. D.M. Stefanescu: *ISIJ Int.*, 1995, 35, 637-650.
13. M. Castro, P. Roquet, R. Castilla, E.Codina: Industrial requirement for melting (Flexicast report, 2013)
14. Thermal Analysis Software. ProserviceTechnology. <http://www.proservicetech.net>
15. D. Gurgul, A. Burbelko, E. Frás, E. Guzik: *Archives of Foundry Engineering*, 2010, 10, 35-40.
16. M. Rappaz: *ESI Conference EUROPAM*, Mainz, 2003.

## Acknowledgements

The research was partially supported by 7FP-2012-7-NMP-ICT-FoF-314540 FLEXICAST project